Molecular Biology of the Cell
Vol. 15, 1134–1145, March 2004

EFA6, Exchange Factor for ARF6, Regulates the Actin Cytoskeleton and Associated Tight Junction in Response to E-Cadherin Engagement

Frédéric Luton,*† Stéphanie Klein,* Jean-Paul Chauvin,‡ André Le Bivic,‡ Sylvain Bourgoin,§ Michel Franco,* and Pierre Chardin*

*Institut de Pharmacologie Moléculaire et Cellulaire, Centre National de la Recherche Scientifique-Unité Mixte Recherche 6097, 06560 Valbonne, France; ‡Institut de Biologie du Développement de Marseille, Centre National de la Recherche Scientifique-Unité Mixte Recherche 6156, Faculté des Sciences de Luminy, 13288 Marseille cedex 09, France; and §Centre de Recherche en Rhumatologie et Immunologie, Faculté de Médecine, Université Laval, G1V 4G2 Québec, Canada

Submitted October 21, 2003; Revised November 21, 2003; Accepted November 21, 2003
Monitoring Editor: Daniel Goodenough

We addressed the role of EFA6, exchange factor for ARF6, during the development of epithelial cell polarity in Madin-Darby canine kidney cells. EFA6 is located primarily at the apical pole of polarized cells, including the plasma membrane. After calcium-triggered E-cadherin–mediated cell adhesion, EFA6 is recruited to a Triton X-100–insoluble fraction and its protein level is increased concomitantly to the accelerated formation of a functional tight junction (TJ). The expression of EFA6 results in the selective retention at the cell surface of the TJ protein occludin. This effect is due to EFA6 capacities to promote selectively the stability of the apical actin ring onto which the TJ is anchored, resulting in the exclusion of TJ proteins from endocytosis. Finally, our data suggest that EFA6 effects are achieved by the coordinate action of both its exchange activity and its actin remodeling C-terminal domain. We conclude that EFA6 is a signaling molecule that responds to E-cadherin engagement and is involved in TJ formation and stability.

INTRODUCTION

Polarized epithelial cells are characterized by two distinct plasma membrane (PM) domains: the free apical domain exposed to the lumen and the basolateral domain facing the neighboring cells and the basal lamina. These two membrane domains display distinct lipid and protein compositions and are separated by a junctional complex, the tight junction (TJ). The TJ provides a tight seal between cells (barrier function) and prevents mixing of the two surfaces (fence function) (Tsukita *et al*., 2001). On freeze-fracture electron micrographs, the TJ looks like interconnected strands of particles encircling in a continuous manner the most apical zone of the lateral membrane (Stevenson *et al*., 1988; Schneeberger and Lynch, 1992). Occludin was the first integral membrane protein identified to localize specifically to the TJ (Furuse *et al*., 1993). A variety of experimental approaches suggested a role for occludin in controlling the formation of the TJ and their associated functions (Tsukita *et al*., 2001). However, it was later found that null mice for occludin were still capable of forming a functional TJ (Saitou *et al*., 1998). More recently, a new family of integral membrane proteins, named claudins, has been identified that contains at least 24 members. Functional analyses have provided strong evidence that claudins control the paracellular transport (Furuse *et al*., 1998; Tsukita *et al*., 2001). Numerous cytosolic molecules associate with the TJ, among which are the proteins ZO-1 and the closely related ZO-2 and ZO-3 (Stevenson *et al*., 1986; Zahraoui *et al*., 2000). These molecules contain three *P*SD-95, *D*lg, *Z*O-1 (PDZ) homology domains, one *src* homology 3 domain, and one guanylyl kinase-like domain and are believed to act as molecular scaffolds. ZO-1 binds to many proteins, including ZO-2 and ZO-3, occludin, claudins, ZO-1 associated nucleic acid-binding protein, and α-catenin. In addition, the C-terminal domain of ZO-1 binds directly to actin filaments and serves as a bridge between the TJ and the underlying actin cytoskeleton (Mitic and Anderson, 1998).

The mechanisms ruling the de novo formation of the TJ, its final multimolecular organization, and the functional interaction of the different proteins constituting the TJ are poorly known. In epithelial cells, cell-cell contacts are initially triggered by the E-cadherin molecules that form a calcium-dependent homotypic interaction between adjacent cells named the adherens junctions (AJs) (Gumbiner, 1996). At the contact zone, the underlying actin is concomitantly rearranged to reinforce the spatial cue and used as a driving force to strengthen cell-cell adhesion. Subsequently, the TJ proteins would be recruited to the cadherin-mediated cell-cell contacts. Then, the TJ would segregate away apically from the AJ that itself distributes along the lateral membrane in response to a signal produced by the integrin-mediated cell–extracellular matrix interaction that triggers the estab-

Article published online ahead of print. Mol. Biol. Cell 10.1091/mbc.E03–10–0751. Article and publication date are available at www.molbiolcell.org/cgi/doi/10.1091/mbc.E03–10–0751.

† Corresponding author. E-mail address: luton@ipmc.cnrs.fr.

Abbreviations used: AJ, adherens junction; Dox, doxycycline; GAP, GTPase activating protein; GEF, guanine nucleotide exchange factor; IF, immunofluorescence; PH, pleckstrin homology; PM, plasma membrane; RITC, rhodamine B isothiocyanate; TER, transepithelial resistance; Tf-R, transferrin receptor, TJ, tight junction.

lishment of the apico-basal axis of polarity. Finally, the TJ forms a separate junctional complex associated to a dense circumferential ring of actin providing a physical barrier at the boundary between apical and lateral membrane (Drubin and Nelson, 1996). Recently, two evolutionarily conserved complexes have been involved in establishing asymmetry and controlling TJ biogenesis in epithelia. The best characterized complex comprised an atypical protein kinase C (aPKC), Par6, and Par3, which in association with the small G protein Cdc42 regulates the formation of TJ (Izumi *et al*., 1998; Joberty *et al*., 2000; Suzuki *et al*., 2001). The second complex, Crumbs3, Pals1, and pals1-associated TJ protein, better studied in *Drosophila* than in mammalian epithelia, has also been involved in cell polarity establishment (Knust and Bossinger, 2002; Roh *et al*., 2003).

Numerous lines of evidence point to a role of the actin cytoskeleton in regulating the paracellular permeability. Early studies on enterocytes indicated that the perijunctional actin cytoskeleton was capable of ATP-dependent contraction, suggesting that the apical actin cytoskeleton could regulate paracellular permeability (Mooseker, 1985). Pharmacological and genetic studies demonstrated the implication of the myosin light chain kinase in this process, providing a large body of evidence regarding the regulatory role of the actin on TJ-regulated paracellular permeability (Turner, 2000). Among the proteins generally involved in actin organization are the small G proteins, especially the Rho family (Hall, 1998). In Madin-Darby canine kidney (MDCK) cells, the inducible expression of dominant-negative or constitutively active mutants of RhoA, Rac1, and Cdc42 affected dramatically the barrier and fence functions of the TJ, disrupted their morphology, and affected the establishment of cell polarity (Jou *et al*., 1998; Rojas *et al*., 2001). Another family of small G proteins has attracted the attention of cell biologists, the Arf family, which comprised six members in mammalian cells. Arf6, its most divergent member, modulates the organization of the actin cytoskeleton and plays a role in membrane transport at the level of the PM (Chavrier and Goud, 1999). In rat kidneys, ARF6 was detected in the brush border at the apical pole of epithelial cells (Londono *et al*., 1999), and subcellular fractionation suggested that it could be present on apical early endosomes (Marshansky *et al*., 1997). In the polarized epithelial cell line MDCK, Arf6 was also found apically where it has been implicated in clathrin-mediated endocytosis (Altschuler *et al*., 1999). More recently, the overexpression in MDCK cells of the constitutively active Arf6 mutant was found to lead to membrane ruffles and actin rearrangement and to affect the turnover of AJs (Palacios *et al*., 2001, 2002).

Small G proteins are molecular switches turned on and off by two groups of regulatory proteins; the exchange factor (GEF) and the GTPase-activating protein (GAP), respectively. GEFs catalyze the exchange of GDP for GTP converting their cognate small G protein into an active GTP-bound form (Vetter and Wittinghofer, 2001). GEFs are multidomain proteins that comprise the exchange factor domain, a subcellular localization domain (e.g., pleckstrin homology [PH] domain) that will presumably specify the site of activation of the cognate small G protein, and one or several domains allowing for connection to other signaling pathways (Jackson and Casanova, 2000; Schmidt and Hall, 2002). Thus, GEFs seem to be central players connected to multiple signaling pathways along which small G proteins are used as molecular switches. Two GEFs for Arf6 have been identified, ARNO and EFA6A (Frank *et al*., 1998; Franco *et al*., 1999). In vitro studies demonstrated that ARNO is more selective for Arf1, whereas EFA6 is specific for Arf6 (Macia *et al*., 2001). However, in vivo, ARNO and EFA6A may be preferentially used, depending on the cell type, upstream signals of stimulation or different subcellular localization within the cell. Recently, three homologues of EFA6A have been described, including one, named EFA6B, that displays a ubiquitous tissue distribution. EFA6A is expressed in neuronal cells and in the polarized enterocyte cells of the gut epithelium (Derrien *et al*., 2002). The general structure of the EFA6 proteins comprises the catalytic Sec7 domain bearing the exchange activity, a PH domain responsible for its membrane localization and a C-terminal region involved in actin cytoskeleton rearrangement (Franco *et al*., 1999). When overexpressed in fibroblastic cell lines EFA6A and EFA6B induced the formation and localized to structures enriched in polymerized actin such as large membrane ruffles and microspikes on the contact-free PM (Franco *et al*., 1999; Derrien *et al*., 2002). In addition, EFA6A perturbed the membrane trafficking of transferrin (Franco *et al*., 1999). To date, these results suggested that EFA6 might coordinate endocytosis with cytoskeletal rearrangements (Franco *et al*., 1999; Derrien *et al*., 2002). In this study, we investigated the role of EFA6 during cell polarity development in MDCK cells. Our results indicate that EFA6 plays a role in the formation of a functional TJ after E-cadherin–mediated cell-cell adhesion. We show that it exerts its function by stabilizing the actin ring onto which the TJ is anchored. Finally, our data indicate that both the exchange activity and the actin remodeling C-terminal region of EFA6 are necessary.

MATERIALS AND METHODS

Cells and DNA

MDCK-T23 cells stably expressing the tetracycline-controlled transactivator have been described previously (Jou and Nelson, 1998). The cDNAs encoding for EFA6A wild type or its mutants E242K and ΔC flanked with an N-terminal VSV-G tag, hereafter referred to as VSVG-EFA6A, VSVG-EFA6A-E242K, and VSVG-EFA6A-ΔC, respectively (Franco *et al*., 1999), were introduced into the vector pUHD10-3 and expressed under the control of the tetracycline responding element. We only used clonal cell lines. Several clones for each of the constructions have been studied and gave similar results. Cells were passaged in 10-cm dishes and grown on 12-mm, 0.4-μm pore size Transwell polycarbonate filters (Corning Costar, Cambridge, MA) in minimal essential medium (MEM) (Sigma-Aldrich, Saint-Quentin Fallavier, France) supplemented with 5% decomplemented fetal calf serum (Cambrex Bioproducts Europe, Verviers, Belgium), penicillin-streptomycin (Invitrogen, Carlsbad, CA), and in the absence or presence of 20 ng/ml doxycycline (Dox). In all experiments, the expression of VSVG-EFA6A was allowed by growing the cells in the absence of Dox for 48 h before analysis. The medium without calcium (spinner medium) was from Sigma-Aldrich and used supplemented with 2 mM EGTA for the calcium switch assays.

Antibodies and Reagents

Antibodies used in this study are as follows: VSV-G (clone P5D4; Roche Diagnostics, Indianapolis, IN), ZO-1 (clone R40.76; Chemicon, Hampshire, United Kingdom), polyclonal rabbit anti-occludin (Zymed Laboratories, Clinisciences, Montrouge, France), claudin 2 (Zymed Laboratories and Dr. S. Tsukita, Kyoto University, Kyoto, Japan), E-cadherin (clone 3G8; a gift of Dr. W. Gallin, University of Alberta, Edmonton, AB, Canada), gp135 (clone 3F2/D8; a gift from Dr. G. Ojakian, State University of New York Health Science Center, Brooklyn, NY), p58 (clone 6.23.3; a gift from Dr. K. Matlin, Harvard Medical School, Boston, MA), transferrin receptor (Tf-R) (clone H68.4; Zymed Laboratories), sheep polyclonal anti-EGF-R (Abcam, Cambridge, United Kingdom), and anti-actin (Chemicon). The anti-EFA6B polyclonal antibody was raised by immunizing rabbits with the recombinant Sec7 domain of EFA6B (amino acids 591–736) as immunogen. The monoclonal anti-ARF6 antibody 8A6-2 (SYL 6B) was generated and characterized as described previously (Marshansky *et al*., 1997). The Texas-Red and fluorescein-coupled antibodies and phalloidin were from Jackson ImmunoResearch Laboratories (West Grove, PA). [^{14}C]Mannitol was from Amersham France (Orsay, France). The NHS-SS-biotin was from Pierce (Perbio Science, France). The streptavidin-agarose beads were from Zymed Laboratories. Latrunculin B was from Calbiochem (Merck Eurolab, Fontenay-sous-Bois, France). All other reagents and chemicals were from Sigma-Aldrich.

Arf6 Pull-Down Assay

The pull-down assay was adapted from Niedergang *et al.* (2003) by using as a bait a fragment (1–226) of the Golgi-localized γ ear-containing Arf-binding protein 3 (GGA3) fused to glutathione *S*-transferase (GST). After three quick rinses in ice-cold phosphate-buffered saline (PBS), the cells were lysed in 50 mM Tris-HCl, pH 8.0, 100 mM NaCl, 10 mM $MgCl_2$, 1% Triton X-100, 0.05% sodium cholate, 0.005% SDS, 10% glycerol, 2 mM dithiothreitol (DTT), and protease inhibitors (Complete; Roche Diagnostics). Lysates were incubated with 40 μg of GST-GGA3 (1–226) bound to glutathione-Sepharose beads (Amersham France). After 40 min, the beads were washed three times in lysis buffer, and the proteins were eluted by boiling in 30 μl of sample buffer. Equal amounts of proteins of each sample were analyzed by immunoblot by using an anti-Arf6 antibody.

Calcium Switch Assay

Cells were washed once quickly in PBS and three times 10 min under agitation in 2 mM PBS-EGTA. At t = 0, cells were incubated in spinner medium supplemented with 2 mM EGTA with or without Dox. Cells were incubated 6 h under these conditions before the calcium switch was performed by replacing the medium with normal MEM with or without Dox.

Paracellular Transport

Transepithelial resistance (TER) was measured as described previously using duplicates or triplicates for each measure (Jou *et al*., 1998). Results are expressed in ohms per square centimeter after substraction of the TER obtained from a duplicate of empty filters. Rhodamine B isothiocyanate (RITC)-dextran 9 kDa (1 mg/ml) and [^{14}C]mannitol (2.5 μCi/filter; 50 mCi/mmol) were added in the apical chamber (200 μl), and 800 μl of normal medium was added in the bottom chamber. Two hours later, the total amount of RITC-dextran and [^{14}C]mannitol in the basal medium was quantitated using a spectrofluorometer and a gamma counter, respectively. The graphs report the percentage recovered in the basal medium of the total amount of reagent added apically. All experiments were repeated at least three times.

Confocal Immunofluorescence

Cells were fixed by 4% paraformaldehyde on ice for 30 min and extracted with 0.5% Triton X-100, 300 mM sucrose, 10 mM PIPES, pH 6.8, 3 mM $MgCl_2$ for 3 min and rapidly rinsed in PBS-CM (1 mM calcium, 0.5 mM magnesium). Samples were then prepared as described previously (Altschuler *et al*., 1999). Images were processed for presentation using the NIH Image and Adobe Photoshop 6.0 software.

Immunoblot

Samples were resolved on SDS-PAGE, and proteins were transferred onto a nitrocellulose membrane. Membrane blocking and antibody dilutions were done in 5% PBS nonfat dry milk. The proteins were revealed by chemiluminescence (ECL; Amersham France) by using secondary antibodies directly coupled to horseradish peroxidase (Jackson ImmunoResearch Laboratories). Quantitation was performed after scanning of the autoradiograph film of nonsaturing signals and using different time exposures.

Triton X-100 Extraction

Cells grown on 24-mm filters were washed three times in ice-cold PBS-CM. The excised filters were slid cells down into 0.4 ml of extraction buffer (0.5% Triton X-100, 120 mM NaCl, 10 mM Tris, pH 7.5, 25 mM KCl, 1.8 mM $CaCl_2$, 0.1 mM DTT, 0.25 mM phenylmethylsuflonyl fluoride, 0.1 mg/ml DNaseI, 0.1 mg/ml RNase) and agitated on ice for 15 min. Cells were recovered using a rubber policemen and spun at 13,000 rpm at 4°C for 20 min. The supernatant (detergent-soluble fraction) was saved and the pellet (detergent-insoluble fraction) resuspended in 40 μl of SDS buffer (1% SDS, 10 mM Tris, pH 7.5, 2 mM EDTA) and boiled for 5 min. Then 0.36 ml of extraction buffer was added. Equal amounts of proteins of each sample were analyzed by SDS-PAGE and immunoblot.

Endocytosis Assays

Cells grown on 12-mm filters were washed three times in ice-cold PBS-CM and incubated two times 30 min in PBS-CM containing 1 mg/ml NHS-SS-biotin. During this step, the EGF-R, claudin-2, and occludin were biotinylated on the lysine residues present in their extracellular domains, 15 estimated residues in the EGF-R based on the Erb2 canine sequence, two residues (K48 and K157) in claudin 2, and one (K137) in occludin. Cells were then washed, and the biotin was quenched by three quick washes in MEM-BSA (MEM, 0.6% bovine serum albumin [BSA], 20 mM HEPES, pH 7.4, penicillin/streptomycin) supplemented with 50 mM NH_4Cl. The cells were further incubated for different periods at 37°C in MEM-BSA followed by three washes in ice-cold PBS-CM. Except for control samples, cells were treated with glutathione (50 mM glutathione, 50 mM Tris, pH 8.8, 100 mM NaCl, 0.2% BSA, pH 8.6) two times 60 min at 4°C to remove the remaining biotin from the cell surface. Cells were solubilized in lysis buffer (1% Triton X-100, 20 mM HEPES, pH 7.4, 2 mM EDTA 2, 125 mM NaCl 125, 0.2 mM phenylmethylsulfonyl fluoride, and protease inhibitors) for 20 min at 4°C and spun 30 min at 13,000 rpm in a Microfuge. The supernatant was precleared on Sepharose beads, and the biotinylated proteins were recovered after a 60-min incubation with streptavidin-agarose beads. Proteins were eluted by vortexing the beads 10 min at 60°C in equal volume of 100 mM DTT and prepared for SDS-PAGE and immunoblot analysis.

Metabolic Labeling Assay

Cells grown on 12-mm filters were rinsed and starved for 15 min in MEM, 5% dialyzed fetal calf serum, without cysteine/methionine (MEM-Cys-Met) for 20 min at 37°C. The cells were then labeled on a 30-μl drop of MEM-Cys-Met containing a mix of [^{35}S]Cys/Met (66 μCi/filter at 1175 Ci/mmol) for 20 min. After four quick washes in MEM-BSA, the cells were then incubated in MEM-BSA for different periods and rinsed three times quickly in ice-cold PBS-CM. The cells were biotinylated using the NHS-SS-biotin (1 mg/ml) in PBS-CM two times 30 min at 4°C. As for the endocytosis assay, the cells were rinsed and solubilized and the lysates precleared. The proteins were immunoprecipitated using specific antibodies coupled to protein A-Sepharose beads, the immunoprecipitates washed five times in lysis buffer, twice in double distilled H_2O, and the immunocomplexes dissociated by two incubations at 75°C in 1.6% SDS, 8.3% glycerol, 167 mM Tris, pH 6.8, under mild vortexing. The pooled eluates were transferred to a new tube containing 1 ml of lysis buffer and 10 μl of streptavidin-agarose beads and further incubated under head-to-head agitation 1 h at 4°C to recover the biotinylated proteins. After washes, two elutions were performed at 60°C in 10 μl of 100 mM DTT under mild vortexing. The eluted metabolically labeled and biotinylated proteins were resolved by SDS-PAGE, revealed, and analyzed using a PhosphorImager (Fujifilm BAS-1500; Fuji Film, Saint-Quentin en Yvelines, France).

RESULTS

VSVG-EFA6A Expressed in MDCK Cells Localized Apically without Disturbing Cell Polarity

EFA6A fused to an N-terminal VSV-G tag, hereafter referred to as VSVG-EFA6A, was expressed in MDCK cells under the control of the tetracycline-repressible transactivator. Figure 1A shows the time course of expression of VSVG-EFA6A in fully polarized cells grown on filters. VSVG-EFA6A expression reaches a peak at 36 h and is maintained up to 96 h after Dox removal. To date, there is no available antibody that recognizes both the endogenous EFA6B protein and the exogenously expressed VSVG-EFA6A protein, so we were unable to compare directly the respective levels of expression. However, compared with other constructs tagged with VSVG or to other studies with different molecules by using the same expression system in MDCK cells, the VSVG-EFA6A signal is on the low range. We have assessed the activation level of endogenous Arf6 by using a pull-down assay, based on the association of GTP-bound Arf6 and the Golgi-localized γ ear-containing Arf-binding protein 3 (GGA3) (Santy and Casanova, 2001), and previously described (Niedergang *et al*., 2003). In MDCK cells, expressing VSVG-EFA6A (−Dox) the amount of Arf6-GTP was increased by eightfold compared with control cells (+Dox) (Figure 1B).

Confocal immunofluorescence (IF) studies have been performed to localize VSVG-EFA6A in polarized MDCK cells. Figure 1C shows a series of xy sections taken from the most apical part of the cell (apex), at the level of the TJ marked using a specific antibody for ZO-1, just below the TJ (sub-TJ) and at the basal pole of the cell below the nucleus. VSVG-EFA6A is present apically above the TJ but is mostly found at the level of the TJ both at the PM and intracellularly. It is also detected just below the TJ but not all along the lateral membrane. The xz section confirmed that VSVG-EFA6A is predominantly localized at the apical pole of the cells. It is noteworthy that using a specific antibody, the endogenous EFA6B protein was also localized at the apical pole of the cells. Finally, we verified that the expression of VSVG-EFA6A did not perturb the cell polarity because the asymmetric distribution of gp135 and p58, markers for the apical

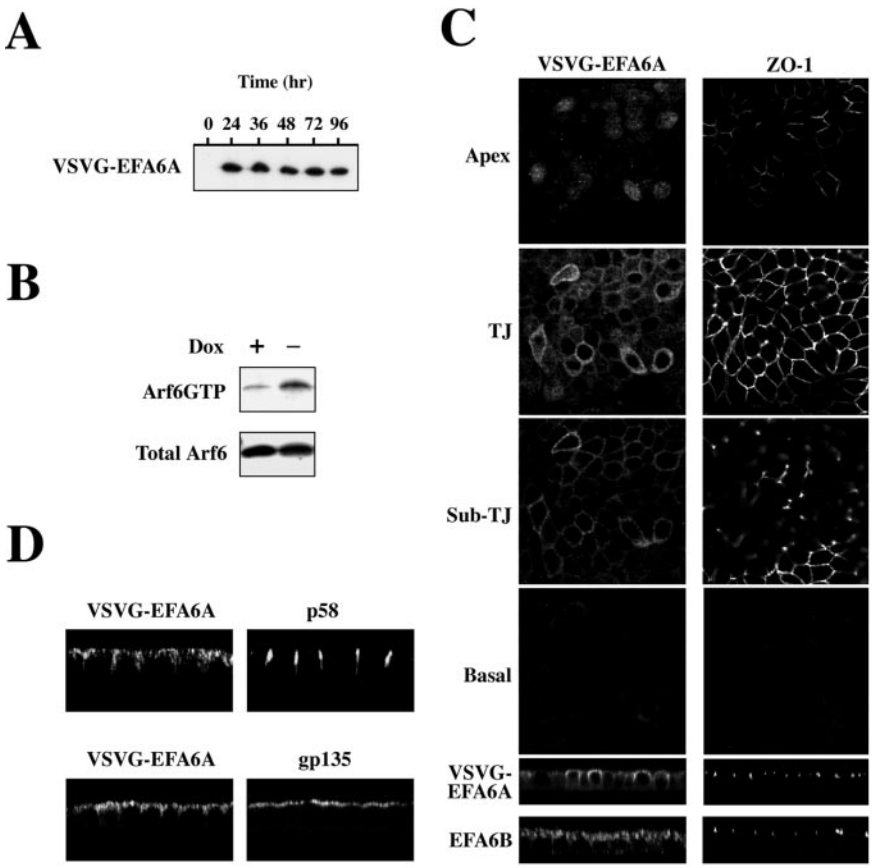

Figure 1. Biochemical and morphological analyses of MDCK cells expressing EFA6A. (A) Kinetic analysis by immunoblot of VSVG-EFA6A expression in MDCK cells after Dox removal. (B) Exogenously expressed VSVG-EFA6A activates the endogenous Arf6 protein. The amounts of GTP-bound endogenous Arf6 from lysates of MDCK-VSVG-EFA6A cells grown with or without Dox (48 h) were determined in a pull-down assay by using GST-GGA3(1-226) (top). Bottom, aliquots of total lysates. (C) Confocal IF analysis of VSVG-EFA6A and ZO-1 localization in MDCK cells expressing VSVG-EFA6A grown in the absence of Dox for 48 h: four xy sections from the apex of the cells to the basal face are shown from top to bottom, and an xz section is presented below. The xz section at the very bottom illustrates the labeling of endogenous EFA6B and ZO-1 in parental MDCK cells. (D) Xz sections of confocal IF images depicting the staining of the basolateral p58 and apical gp135 markers compared with VSVG-EFA6A.

and basolateral membrane domains, respectively, was unaffected (Figure 1D).

VSVG-EFA6A Expression Accelerates the De Novo Formation of a Functional TJ

We assessed the barrier function in polarized MDCK cells expressing VSVG-EFA6A. Measurement of the TER, the paracellular transport of two nonionic molecules, the 9-kDa RITC-dextran and the smaller molecule [^{14}C]mannitol, and freeze fracture electron microscopy failed to show any effect of VSVG-EFA6A expression on the barrier function and general morphology of the TJ in polarized MDCK cells (our unpublished data). Next, we analyzed the effects of VSVG-EFA6A expression on the de novo formation of a TJ. To this end, we made use of the so-called calcium switch procedure (Cereijido *et al.*, 1998; Denker and Nigam, 1998). In this experiment, cell polarity and calcium-dependent E-cadherin cell-cell contacts are disrupted by removing the calcium from the cell culture medium. It is well established that the TJ is also disassembled upon calcium removal. Once the cells have completely lost all their cell-cell contacts, calcium is added back triggering the homotypic E-cadherin interaction. Subsequent to the E-cadherin engagement, one can follow the de novo formation of the TJ and the development of cell polarity. In Figure 2, fully polarized MDCK-VSVG-EFA6A cells grown in the presence or absence of Dox (48 h) were submitted to a calcium switch and the paracellular permeability assessed over time. After readdition of calcium the TER increased slowly except for the cells expressing VSVG-EFA6A (−Dox), in which the TER developed very rapidly to reach a maximum after 4 h at ~200 ohms · cm^{-2} (Figure 2A; our unpublished data). Over time, the control cells (MDCK-T23 +/− Dox and MDCK-VSVG-EFA6A +Dox) reached the same plateau confirming that once the cells are polarized EFA6A does not affect their TER (Figure 2A). We also examined the paracellular transport of the nonionic molecules 9-kDa RITC-dextran and [^{14}C]mannitol. The cells were submitted to a calcium switch and then the tracer molecules were added apically at different times after calcium addition. Figure 2, B and C, reports the results obtained 2 h after calcium addition. In control cells (MDCK-T23 +/−Dox and MDCK-VSVG-EFA6A +Dox), ~40% of dextran or mannitol were recovered in the basal medium. However, in MDCK cells expressing VSVG-EFA6A (−Dox) only ~5% of dextran and 25% of mannitol had diffused to the basal medium, indicating that the junctional barrier had closed faster.

We further examined the formation of the TJ by confocal IF by following occludin and ZO-1. After a calcium switch, control cells translocated the two TJ proteins at cell-cell contact areas in a coordinated manner to eventually form a classic-looking TJ structure after 16 h (Figure 2D, top). In cells expressing VSVG-EFA6A, the quantity of occludin and ZO-1–detected at cell-cell contacts is found to be increased at 1 h after calcium addition and becomes even more evident after 2 h (Figure 2D, bottom). Thus, the TJ is formed faster but is ultimately indistinguishable from control cells. Claudin 2, the most abundant claudin member in MDCKII, behaved as occludin and ZO-1 (our unpublished data). Note, that the faster apparition of TJ proteins is temporally correlated with the recovery of the barrier function (Figure 2A). We conclude that expression of VSVG-EFA6A in MDCK cells accelerates the formation of a functional TJ.

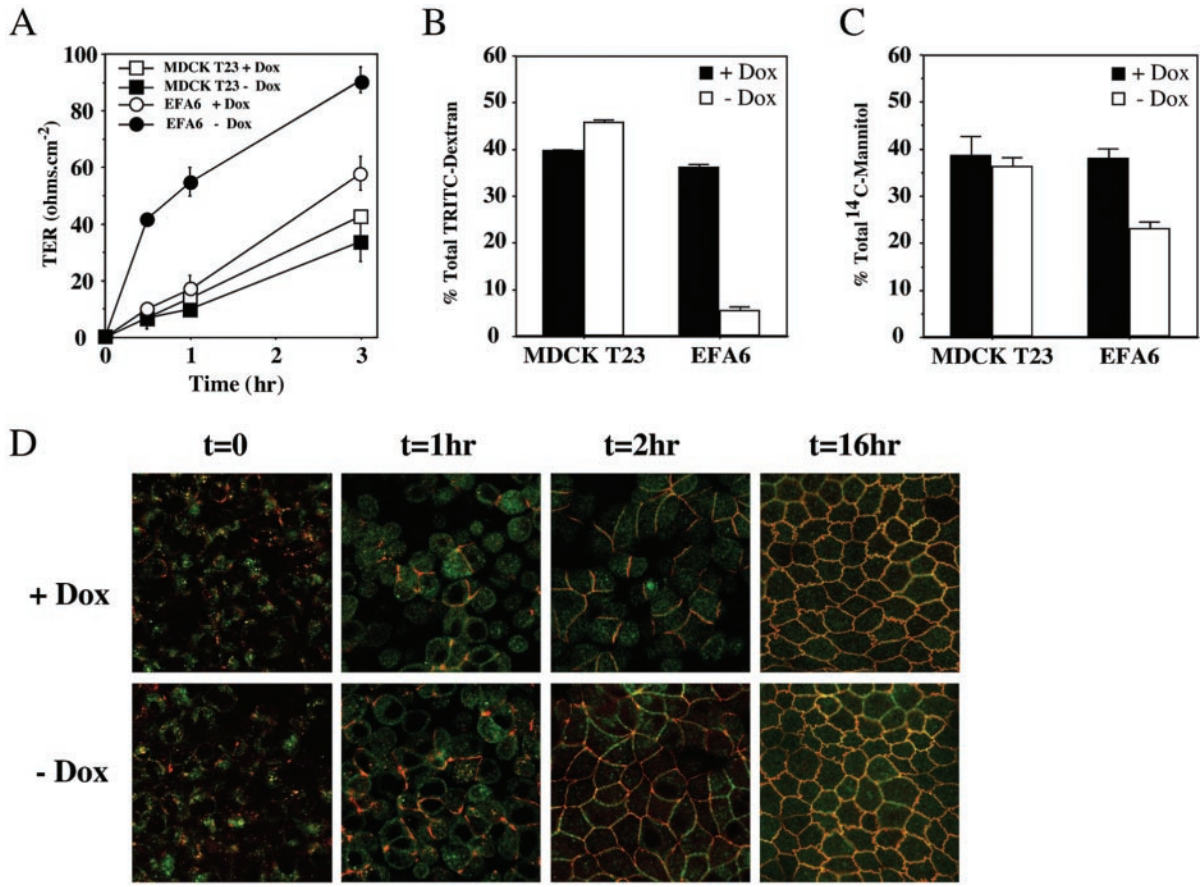

Figure 2. EFA6A expression accelerates the formation of a functional TJ. Cells were submitted to calcium starvation for 6 h followed by the addition of calcium. The indicated cell monolayers were analyzed for their TER (A), 9-kDa-dextran RITC paracellular diffusion (B), [^{14}C]mannitol paracellular diffusion (C). (D) Confocal IF analysis at the TJ of MDCK-VSVG-EFA6A cells grown in the presence or absence of Dox (48 h). Cells were stained for occludin (green) and ZO-1 (red).

E-Cadherin Engagement Induces a Transient Increase of the Level of EFA6 and Its Translocation to the PM before the Formation of TJ

It has long been shown that, after calcium addition during a calcium switch procedure, TJ proteins are transported to the PM where they associate with the cortical actin cytoskeleton as judged by their partitioning into the detergent-insoluble fraction. We inspected the Triton X-100 partitioning of occludin and VSVG-EFA6A by immunoblots. On incorporation into TJ, occludin was shown to be phosphorylated and to migrate on SDS-PAGE as several bands of 66 kDa and higher molecular weights (Sakakibara *et al*., 1997; Wong, 1997). In Figure 3A, we noticed an increase of occludin phosphorylation and partitioning into the detergent-insoluble fraction readily visible 4 h after the addition of calcium. Eventually, it reached a partition similar to the one of fully polarized cells after an overnight incubation. On calcium addition, the quantity of VSVG-EFA6A protein increased very quickly to peak at 2 h but decreased also rapidly to normal level after 4 h (Figure 3A). Interestingly, the increase in VSVG-EFA6A protein occurs concomitantly with the apparition of 6% of the protein into the detergent-insoluble fraction, consistent with its association with the actin cytoskeleton. This is also accompanied by its translocation to the PM visualized by IF (our unpublished data). At steady state, VSVG-EFA6A was never found in the detergent-insoluble fraction even when high amounts of proteins were analyzed and aurodiographs exposed for a long time. The quantity of EFA6A present in the detergent-insoluble fraction could be underestimated due to a weak and/or a transient interaction with the actin cytoskeleton. Compared with occludin, we find that the increased level of VSVG-EFA6A protein and its apparition in the detergent-insoluble fraction precedes temporally the incorporation of occludin into the TJ as judged by phosphorylation. This is consistent with our observation that EFA6A acts on the formation of the TJ.

The calcium switch assay assumes that the effects observed are directly through calcium-dependent E-cadherin homotypic interactions at the AJ. We sought to verify that in response to calcium the increased expression of VSVG-EFA6A was directly dependent on E-cadherin engagement, rather than through secondary effects of calcium. To this aim, the cells were submitted to a calcium switch in the absence or presence of E-cadherin blocking antibodies in the extracellular medium, and the amount of VSVG-EFA6A was analyzed by immunoblots. We observed that the increase in VSVG-EFA6A in response to calcium addition was completely inhibited when E-cadherin blocking antibodies were added in the calcium-containing medium (Figure 3B). In contrast, control antibodies specific for the apical membrane marker gp135 had no effect. We also analyzed the fate of the endogenous EFA6B protein during the calcium switch experiment in normal MDCK cells. We observed an increase in expression of the protein that was even greater than the one

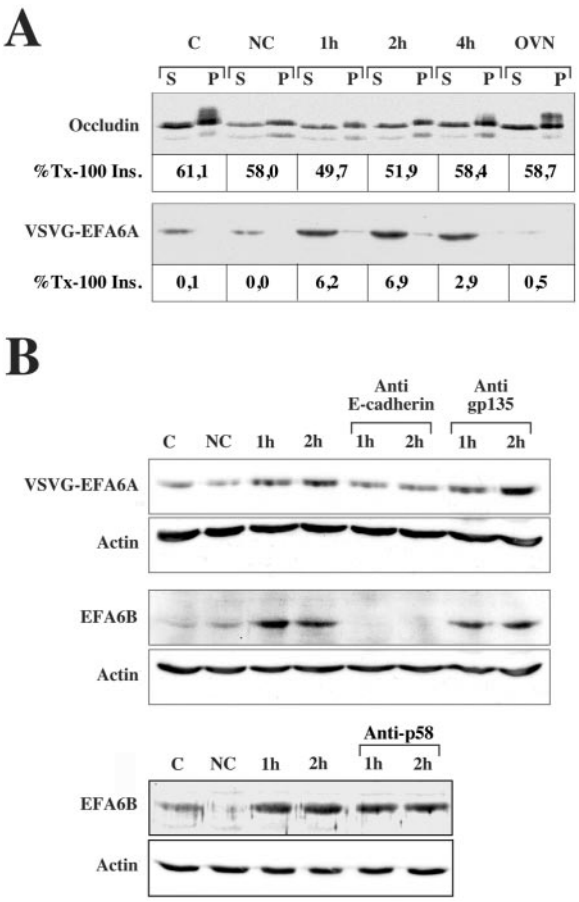

Figure 3. EFA6 responds to E-cadherin engagement before TJ formation. (A) VSVG-EFA6A and occludin Triton X-100 partitioning during calcium switch analyzed by immunoblots. The percentages of the Triton X-100–insoluble fraction of occludin and VSVG-EFA6A measured by densitometric analysis are indicated below the immunoblots. (B) Immunoblot analysis of the level of expression of VSVG-EFA6A detected with the anti-VSVG–specific antibody, and of the endogenous EFA6B protein detected with a rabbit-specific antiserum, in response to E-cadherin engagement. The same amount of proteins was loaded in each lane and controlled by anti-actin immunoblot of the corresponding gels. C, control cells grown in normal calcium medium; NC, cells incubated in the absence of calcium for 6 h; 1 and 2 h, time after calcium addition after the 6-h calcium depletion period. When indicated, the antibodies were added with the calcium.

observed with the exogenously expressed EFA6A and that was completely blocked by anti-E-cadherin antibodies as well. Once again, control antibodies specific for gp135 or the basolateral membrane marker p58 had no effect. A portion of EFA6B was also found in the Triton X-100–insoluble fraction during the calcium switch (our unpublished data). These results demonstrated that EFA6 responds to E-cadherin engagement upon cell-cell contact initiation to participate in the formation of the TJ.

The Accelerated Formation of Functional TJ Is Dependent on Both the Nucleotide Exchange Activity and the Actin Remodeling C-Terminal Domain of EFA6A

Because EFA6 molecules possess two separate active domains, we set out to determine which from the nucleotide exchange activity and/or actin-remodeling C-terminal region was necessary to promote TJ biogenesis. We made two additional MDCK cell lines, one expressing VSVG-EFA6A containing a point mutation of the conserved glutamic acid within the Sec7 domain essential for the exchange activity and one deleted of the C-terminal tail that conserves the PH domain responsible for the membrane localization. Both mutants were expressed under the tetracycline-repressible promoter and their level of expression examined by immunoblot (Figure 4A). The two mutated proteins localized essentially apically in a pattern similar to the one of the wild-type protein, with some additional intracellular staining for the C-terminal truncated form (EFA6A-ΔC) (our unpublished data). The two mutants were tested for their effect on the de novo formation of TJ after a calcium switch as performed in Figure 3. Compared with VSVG-EFA6A, it is apparent that neither mutant was capable of accelerating TJ assembly monitored either by TER (Figure 4B) or RITC-dextran 9-kDa diffusion (Figure 4C). We also determined whether the two EFA6A mutants could respond to E-cadherin engagement. In both cell lines, the level of expression of the mutated EFA6A increased upon calcium switch (Figure 4D). This suggests that the inability of the two mutants to affect the TJ biogenesis was not due to their incapacity to respond to E-cadherin engagement but rather to their inability to transduce the signal further. These results indicate that both the Sec7 and C-terminal domains of EFA6 are necessary, perhaps by acting in a coordinated manner, to regulate the assembly of the TJ downstream of E-cadherin–mediated cell-cell contact.

VSVG-EFA6A Delays the Loss of Barrier Function and Disassembly of TJ upon Calcium Removal

There are many examples of pharmacologically and physiologically induced alterations in paracellular permeability revealing the dynamic organization of the TJs (Cereijido *et al*., 1998; Nusrat *et al*., 2000). The molecular mechanisms at the basis of this dynamic are largely unknown; however, it is most likely that they participate in the de novo formation of TJ during cell polarity development. Because we observed an acceleration in the assembly of the TJ in MDCK cells expressing VSVG-EFA6A, we suspected that the turnover and/or interactions of the TJ proteins was also altered when those cells were polarized. We tested this hypothesis by looking at the disassembly of TJs in response to calcium removal. First, we measured over time the TER after calcium depletion from fully polarized cells. We observed that VSVG-EFA6A–expressing cells were slower to loose their electrical resistance than the control cells, indicating that the TJ were more difficult to disassemble in those cells (Figure 5A). Second, we examined the paracellular diffusion of the RITC-dextran 9-kDa molecule. One hour after calcium removal, we measured that in control cells an average of ≈50% of dextran had diffused through the monolayer into the basal medium. The diffusion was only of ≈25% in VSVG-EFA6A cells (Figure 5B). These functional results were confirmed by confocal IF where we observed a slower loss of ZO-1 and occludin staining in VSVG-EFA6–expressing cells temporally correlated with the loss of paracellular diffusion (our unpublished data). These experiments demonstrated that in fully polarized cells expressing VSVG-EFA6A, even though the morphology and barrier function of the TJs seemed normal, the TJs were altered and more stable than in control cells.

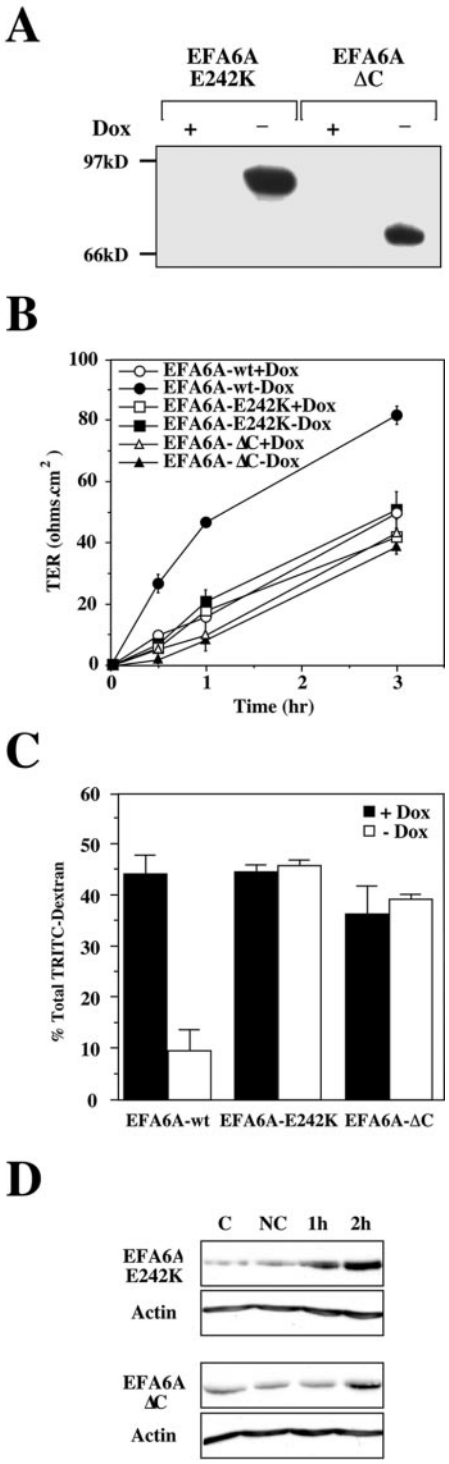

Figure 4. Exchange activity and the C-terminal actin remodeling domains of EFA6A are required to accelerate TJ formation. (A) Expression of VSVG-EFA6A-E242K and VSVG-EFA6A-ΔC in MDCK cells were analyzed by immunoblot by using the anti-VSVG antibody. Cells were submitted to a calcium switch and were analyzed for TER (B) and 9-kDa-dextran RITC paracellular diffusion (C). (D) Immunoblot analysis of the level of expression of the mutated proteins detected with the anti-VSVG–specific antibody in response to E-cadherin engagement. The same amount of proteins was loaded in each lane and controlled by anti-actin immunoblot of the corresponding gels. C, control cells grown in normal calcium medium; NC, cells incubated in the absence of calcium for 6 h; 1 and 2 h, time after calcium addition after the 6-h calcium depletion period.

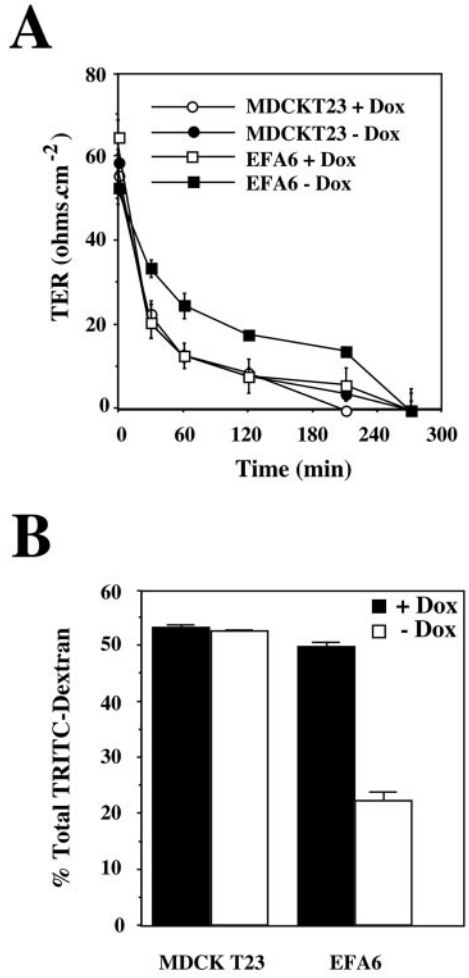

Figure 5. EFA6A delays the disassembly of TJ. The indicated cell monolayers were analyzed for their TER (A) and (RITC)-dextran 9-kDa paracellular diffusion (B) during TJ disassembly upon calcium removal.

VSVG-EFA6A Promotes the Retention of TJ Proteins at the PM

Our current data suggest a role for EFA6 in TJ formation and stabilization, whereas previous data demonstrated a role for EFA6 in actin cytoskeleton organization (Franco *et al*., 1999; Derrien *et al*., 2002). The earliest morphological event in response to E-cadherin engagement is a localized reorganization of the actin cytoskeleton (Drubin and Nelson, 1996). Therefore, we propose that the effects of EFA6A on the acceleration of the assembly or on the delay of the disassembly of the TJ is through the selective retention of TJ proteins at the cell surface, perhaps by virtue of the TJ association with the cortical actin cytoskeleton. To test this hypothesis, we compared the rate of delivery and half-life of occludin and Tf-R at the PM. Cells were labeled with the mix [^{35}S]Cys/Met for 20 min and chased for different periods of time after which they were cooled down and their cell surface biotinylated. The cells were then lysed and the biotinylated proteins isolated, first by immunoprecipitation with a specific antibody and then, after immunocomplex dissociation, after streptavidin bead precipitation. After elution, the radiolabeled biotinylated proteins were separated on SDS-PAGE, detected, and quantitated with a Phospho-

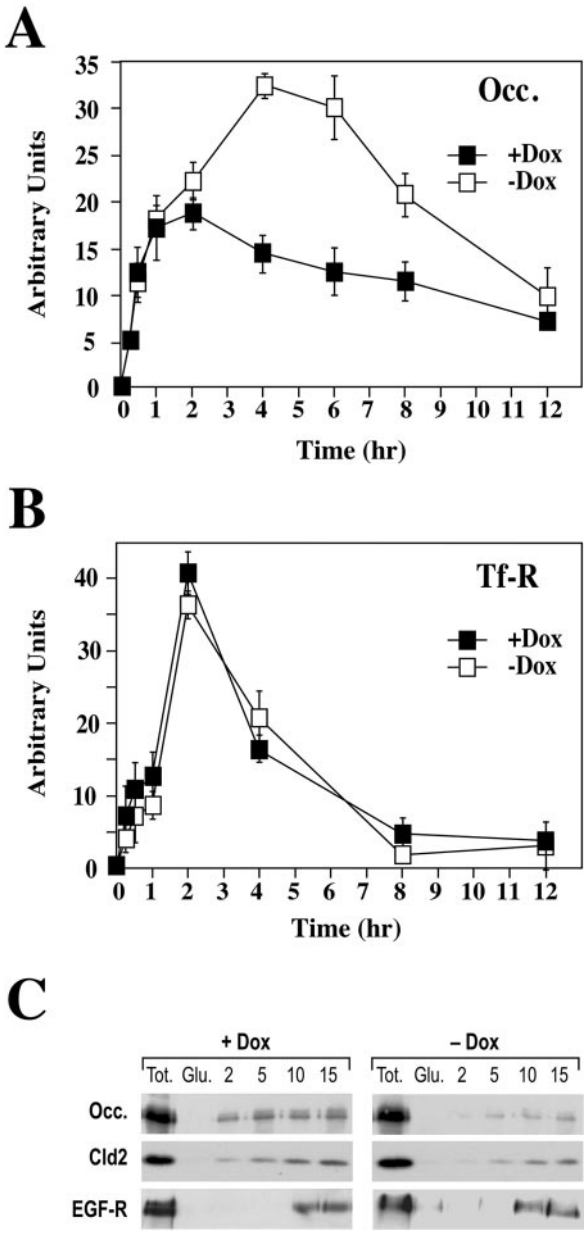

Figure 6. EFA6A promotes the cell surface retention of TJ proteins. The quantity of occludin (A) and Tf-R (B) present at the PM of MDCK-VSVG-EFA6A cells grown in the presence or absence of Dox (48 h) were determined by pulse-chase and cell-surface biotinylation (for details, see MATERIALS AND METHODS). The amounts of protein were quantified by densitometry and plotted against time. (C) Biotinylation endocytosis assay of MDCK-VSVG-EFA6A cells grown in the presence or absence of Dox (48 h) for occludin, claudin 2, and the EGF-R (for details, see MATERIALS AND METHODS). Immunoblots for the total amount of biotinylated protein (Tot.), the control for glutathione stripping after biotinylation (Glu.), the protected amount of proteins from glutathione stripping after 2-, 5-, 10-, and 15-min internalization were quantified by densitometry and plotted against time.

rImager. The rate of delivery is calculated from the slope of the curve at early time points before the plateau is reached. By analyzing several time points early on during the chase, we could determine that the rates of cell surface delivery of occludin (Figure 6A) and Tf-R (Figure 6B) were unaffected by the expression of VSVG-EFA6A. In contrast, later time points inform us about the duration that the proteins remain at the PM. In control cells, the maximum amount of occludin at the PM was detected after 2 h. In cells expressing VSVG-EFA6A, the total amount of protein was higher and the time at which the peak was reached was later (Figure 6A). Because the rates of protein synthesis (our unpublished data) and PM delivery were comparable in both cell groups, the differences observed can only be explained by an increased retention of occludin at the cell surface. In contrast, the length of time spent by the Tf-R at the cell surface was unaffected by VSVG-EFA6A expression (Figure 6B).

A direct consequence of the cell surface retention of occludin should be a concomitant decrease in its rate of endocytosis. This was addressed by cell surface biotinylation and protection of the biotinylated proteins from the reducing agent glutathione over the course of their internalization from the PM. We analyzed the endocytosis of occludin and claudin 2. Indeed, VSVG-EFA6A–expressing cells showed a slower rate of endocytosis of both occludin and claudin 2 (Figure 6C). The quantitative analysis of five independent experiments indicated that after 15 min, 34.5 and 36% of occludin and claudin 2 were internalized, respectively, in control cells, whereas only 12 and 10.5%, respectively, were internalized in cells expressing VSVG-EFA6A. However, the endocytosis of two other basolateral membrane proteins, the EGF-R, 32.5% for control cells versus 31% for cells expressing VSVG-EFA6A (Figure 6C) and the polyimmunoglobulin receptor (our unpublished data), were unchanged. These results indicate that expression of VSVG-EFA6A promotes the selective cell surface retention of the TJ proteins and their exclusion from endocytic pathways.

VSVG-EFA6A Enhances the Anchorage of the TJ Proteins by Accelerating the Polarized Reorganization of the Actin Cytoskeleton

Next, we tested whether VSVG-EFA6A influenced the asymmetric reorganization of the actin cytoskeleton after a calcium switch. In VSVG-EFA6A–expressing cells, as early as 30 min after calcium addition we observed more cell-cell contacts enriched in polymerized actin and labeled for ZO-1 than in control cells (our unpublished data). After 3 h, the VSVG-EFA6A cell monolayer already had the honeycomb morphology with a strong actin staining at the level of the TJ and the presence of microvilli characterized by the punctate apical staining of actin (Figure 7A). The difference with control cells became less evident after 5 h and was no longer detectable after 16 h (our unpublished data). We noticed that the advanced polarized rearrangement of the actin cytoskeleton correlates temporally with the accelerated TJ assembly (Figure 2) and VSVG-EFA6A increase of expression (Figure 3).

This result indicated that EFA6 might act by stabilizing the actin ring, supporting the TJ. We examined the sensitivity of the actin cytoskeleton to latrunculin B by confocal IF. The mode of action of this drug makes it a very useful tool to analyze the stability of actin cytoskeleton structures. It does not depolymerize actin but instead sequesters free G-actin released accordingly to the turnover of actin structures, making it unavailable for the de novo polymerization of actin filaments (Spector *et al.*, 1983; Gronewold *et al.*, 1999). Figure 7B shows xy sections of MDCK cell monolayers treated 15 min with 5 μM latrunculin B and subsequently stained for actin and ZO-1. The most sensitive actin structures were the basal stress fibers and the lateral cortical actin, which disappeared very quickly in both cell monolayers. Note, that after latrunculin treatment some phalloidin

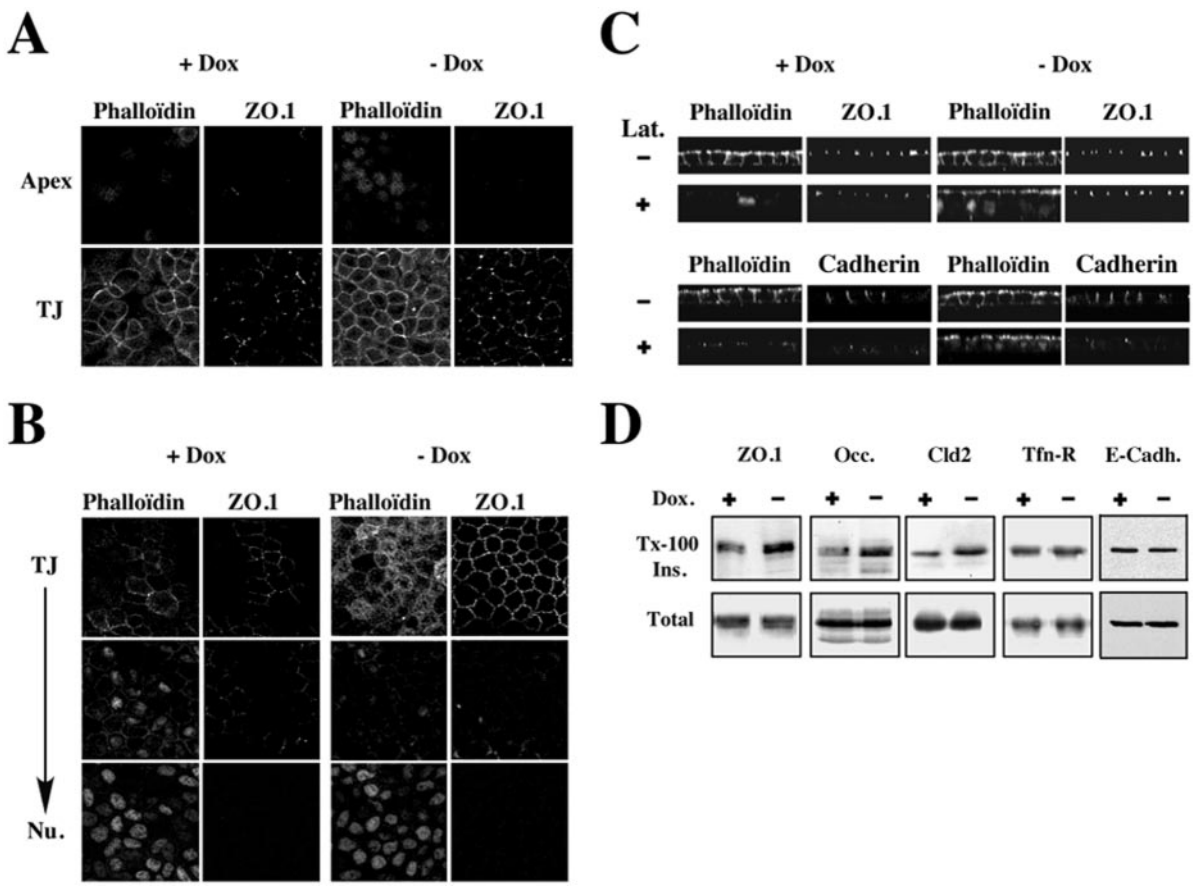

Figure 7. EFA6A accelerates the polarized reorganization of the actin cytoskeleton and anchorage of the TJ proteins. (A) Confocal analysis of actin and ZO-1 during a calcium switch of MDCK-VSVG-EFA6A cells grown in the presence or absence of Dox (48 h). Single xy sections taken at the level of the cell-cell contacts and at the apex of the cells are shown 3 h after calcium addition. (B) Confocal analysis of actin and ZO-1 in polarized MDCK-VSVG-EFA6A cells grown in the presence or absence of Dox (48 h) after a 15-min treatment with latrunculin B (5 μM). Single xy sections taken at the TJ, sub-TJ, and nuclei levels are shown. Two independent xz sections are presented at the bottom. (C) Xz sections of confocal IF analysis of actin and ZO-1 (top) or actin and E-cadherin (bottom) in polarized MDCK-VSVG-EFA6A cells grown (+/− Dox 48 h) after or not a 15-min treatment with latrunculin B (5 μM) (Lat. +/−). (D) Immunoblot analysis of the total amount or the Triton X-100–insoluble fraction of ZO-1, occludin, claudin 2, Tf-R, and E-cadherin in polarized MDCK-VSVG-EFA6A cells grown in the presence or absence of Dox.

staining is visible in the nucleus. In control cells, we could also observe a significant decrease of the actin staining at the level of the apical microvilli as well as the actin ring, supporting the TJ. Concomitantly, we observed that the staining for ZO-1 was also diminished (Figure 7B). In comparison, VSVG-EFA6A expressing cells demonstrate strong apical actin and ZO-1 staining. These data show that the expression of VSVG-EFA6A results in the stabilization of the apical actin cytoskeleton structures.

Adherens junctions present all along the lateral membrane are mostly found concentrated just below the TJ at the level of the thick actin ring surrounding polarized cells. We asked whether EFA6 could also stabilize the AJ. Figure 7C shows xz sections of monolayers grown in the presence or absence of Dox, exposed or not to latrunculin B and labeled for actin and ZO-1 or E-cadherin. As shown above, the actin and TJ staining were identical in cells expressing or not VSVG-EFA6A, but after the latrunculin treatment, only the cells expressing VSVG-EFA6A retained a marked apical actin and ZO-1 staining (Figure 7C, top). In control cells treated with latrunculin, the actin staining was more reduced that the one of ZO-1. This is probably due to the fact that at intersecting points of multiple cell contacts the strong knot of polymerized actin is less affected and concentrates the associated ZO-1. The E-cadherin staining was indistinguishable whether the cells were grown in the presence or absence of Dox (48 h). However, in contrast with TJ, AJs were sensitive to latrunculin whether the cells expressed VSVG-EFA6A or not, as the E-cadherin staining disappeared in both monolayers (Figure 7C, bottom). Nevertheless, the apical actin staining was still protected in cells expressing VSVG-EFA6A. This result suggests that EFA6 strengthens the apical actin ring into which the TJ is anchored but not the AJ-associated actin structure.

If VSVG-EFA6A expression promoted a greater retention of the TJ proteins at the PM through actin anchoring, it should be reflected by an increase of the amount of TJ proteins within the detergent-insoluble fraction. We therefore compared the Triton X-100–partitioning of the TJ proteins in polarized cells (Figure 7D). VSVG-EFA6A–expressing cells displayed an increased partitioning of ZO-1, occludin, and claudin 2 into the detergent-insoluble fraction with a similar factor of enrichment of 1.8 ± 0.2, whereas the total amounts of each protein were unchanged (bottom). This increase was specific as the partitioning of the Tf-R or E-cadherin was unaffected. We conclude that VSVG-EFA6A

expression stabilizes selectively the apical actin cytoskeleton and facilitates a better anchorage of TJ proteins, and thus the formation of functional TJ during cell polarity development.

DISCUSSION

We investigated the role of EFA6 in epithelial cells during the development and maintenance of cell polarity. Our studies identified EFA6 as an important signaling molecule recruited upon E-cadherin engagement and involved in coordinating the organization of the apical actin cytoskeleton, which leads to an enhanced stability and accelerated assembly of the TJ. We made the initial observation that expression of EFA6A in MDCK cells accelerates at early stages the de novo formation of actin cytoskeleton and a functional TJ. Subsequently, we show that EFA6A promotes the cell surface retention of TJ proteins and their exclusion from endocytic pathways. Finally, we show that the TJ and the actin-ring onto which it is anchored are more stable and less sensitive to disassembly in response to calcium depletion or latrunculin treatment. We conclude that EFA6 recruitment by E-cadherin engagement contributes to the establishment of cell polarity by strengthening the actin cytoskeleton to generate a retention domain onto which the TJ molecules are stably anchored. Furthermore, our results show that EFA6 exerts these effects through both its exchange activity and actin-remodeling C-terminal domain.

After we started our study, three close homologues of EFA6A were described forming a distinct GEF family (Derrien *et al*., 2002). The prototypic clone used in our study, named EFA6A, is brain and intestine specific. EFA6B is broadly expressed except in the brain, whereas EFA6C and EFA6D are found mostly in the brain, although EFA6D might also be present in some epithelial tissues. Only EFA6A and EFA6B have been well characterized. Both proteins are very homologous and share a highly conserved Sec7, PH, and C-terminal domain. EFA6B stimulates nucleotide exchange on Arf6 and promotes actin remodeling through its C-terminal region in a manner indistinguishable from that of EFA6A. In addition, our study shows that the endogenous EFA6B and exogenous EFA6A both localize apically and respond to E-cadherin engagement (Figure 4; see below).

EFA6: Exchange Factor for Arf6 and Actin Cytoskeleton-regulating Protein

Two studies from the same laboratory indicated that overexpression of the GTP-bound mutant of Arf6, Arf6-Q67L, in MDCK cells resulted in the disassembly and down-modulation of the AJ (Palacios *et al*., 2001, 2002). We have also analyzed the effects of Arf6-Q67L overexpression and found analogous results, namely, a faster rate of TJ disassembly upon calcium depletion measured by TER and nonionic molecules diffusion (Klein, manuscript in preparation). How can we reconcile these results with those of EFA6 that retarded disassembly under those conditions? One explanation is that the mutation Q67L blocks the GDP-GTP cycle, whereas the overexpression of EFA6 will lead to the opposite effect, that is, a greater amount of GTP-bound Arf6 fully capable of cycling between the GTP- and GDP-bound forms. A better Arf6 mutant to mimic EFA6 effects would be the fast cycling Arf6-T157A that occurred in vivo to be more active than the Arf6-wt protein. Indeed, in HeLa cells Arf6-T157A induced, similarly to EFA6, the formation of large membrane ruffles accompanied with actin rearrangements where it localized (Santy, 2002). In contrast, HeLa cells overexpressing Arf6-Q67L have a very round morphology and smooth edges with only few short membrane projections (Radhakrishna *et al*., 1996; Santy, 2002). Furthermore, EFA6, like all the other GEFs, is not exclusively an exchange factor but displays another function that contributes to the phenotype we observed. As mentioned above, it is well established that EFA6 C-terminal domain induces dramatic rearrangements of the actin cytoskeleton, promoting the formation of long actin-based membrane extensions, in a manner independent of EFA6 GEF activity (Franco *et al*., 1999; Derrien *et al*., 2002). In our study, we have used two EFA6 mutants to address the contribution of the Arf6-GEF activity and the actin remodeling C-terminal domain. Neither mutant could carry out the effects of the wild-type protein. We have nonetheless shown that both mutants were responding to E-cadherin engagement (Figure 5). It suggests that it is the coordinated action of the exchange activity (Arf6 activation) and the C-terminal domain (actin organization) that contributes to the accelerated formation of the TJ.

One could have expected the mutants to act as dominant negative proteins either by saturating the sites of EFA6 localization, by competition for the substrate Arf6, or by forming an abortive complex with Arf6. There are several possible explanations for the absence of a dominant negative phenotype: 1) Massively overexpressed exogenous EFA6A by transient transfection in fibroblastic cell lines is still found localized at the PM, as the endogenous protein, indicating that the sites of association at the PM are difficult to be saturated. This would be especially true at the low level of expression of EFA6A in our cell system expression. 2) Because EFA6 acts enzymatically, the competitive effect of the transfected mutant would need to be extensive to abolish completely the activity of the endogenous EFA6 and to observe a loss-of-function. Our moderate cell expression system might not provide such conditions. 3) In addition, during the calcium switch the level of endogenous protein increases dramatically, further reducing the competitive effect of the exogenous protein. 4) The exogenous EFA6 does not form a stable complex that sequesters its substrate, i.e., Arf6; therefore, the endogenous Arf6 remains available to the endogenous EFA6. In any case, the absence of phenotype obtained with the mutants suggests that both the exchange activity and C-terminal domain of EFA6 are necessary to regulate the TJ.

Arf6 has been shown to modulate membrane transport at the cell surface (Chavrier and Goud, 1999). We reasoned that Arf6 activation might contribute to the accelerated formation of TJ in cells expressing EFA6A by promoting the transport of TJ proteins to the cell surface. However, our pulse-chase experiments followed by cell surface biotinylation clearly show that the rate of transport of occludin to the PM was not affected. Although, one cannot totally exclude a contribution of Arf6 by influencing membrane transport, we would rather favor the hypothesis that Arf6 acts on the organization of the actin cytoskeleton in a coordinated manner, yet independent, with the C-terminal domain of EFA6.

EFA6 Is Acting Downstream of E-Cadherin

The development of cell polarity is initiated by E-cadherin homotypic interactions between adjacent cells and results in the localized reorganization of the actin cytoskeleton that serves to recruit signaling molecules to reinforce the E-cadherin signal leading, among others, to TJ formation (Drubin and Nelson, 1996). We propose that EFA6 is acting primarily directly on the TJ rather than indirectly through an effect on the AJ. This is supported by the observation that the expression of EFA6A affects the TJ in polarized cells that have not been submitted to a calcium switch and the fact

that E-cadherin, in contrast with ZO-1, is equally sensitive to the latrunculin treatment regardless of the expression of VSVG-EFA6A. Furthermore, in response to calcium, we observed an increase of EFA6 (exogenous and endogenous) level of expression, the apparition of EFA6 in the Triton X-100–insoluble fraction, indicative of its association with the actin cytoskeleton, and its translocation to the PM by confocal IF. E-cadherin–specific blocking antibodies abolished the increase of EFA6 in response to calcium, as well as its translocation to the PM (Figure 4; our unpublished results), indicating that EFA6 recruitment results from E-cadherin engagement. However, at this point it is not possible to rule out a direct effect of EFA6 on the AJ. Subtle changes, experimentally undetectable, on the turnover of the AJ might affect TJ assembly. One can envision a model in which EFA6 would affect in return E-cadherin–mediated cell-cell junction to balance adhesion signaling and polarity development and/or establishment.

As mentioned above, after calcium addition the levels of exogenous EFA6A increase rapidly. Because EFA6A transcription is under the control of a heterologous artificial promoter, it suggests that the total cellular amount of EFA6A protein is modulated by either its rate of translation or its rate of degradation. Metabolic labeling experiments indicated that the turnover of EFA6A is very rapid with a half-life of only 25 min and a rate of protein synthesis 5 and 10 times faster than the one of occludin and Tf-R, respectively (our unpublished data). Such a rapid turnover could allow for a swift regulation of its expression level by controlling its rate of degradation.

EFA6 Participates in the Development and Maintenance of the TJs by Acting on Their Association with the Actin Cytoskeleton

Our experiments with latrunculin indicate that EFA6A expression stabilizes selectively the apical actin cytoskeleton onto which the TJ proteins are associated. This effect could be mediated through multiple pathways controlling the actin: increased expression, massive local redistribution, increased actin polymerization or reduced actin depolymerization. By immunoblot, we did not detect any difference in the overall amount of actin or a clear difference by IF in the intracellular actin distribution or for that matter apical actin staining (our unpublished data). Although one cannot exclude that EFA6 accelerates the rate of actin polymerization, the molecular mechanism by which the latrunculin B acts would rather suggest that EFA6 stabilizes the apical polymerized actin by slowing down its depolymerization.

Beside strengthening cell-cell adhesion and recruiting signaling molecules, one proposed role for the actin cytoskeleton during the development of cell polarity is to restrict the distribution of proteins at the contact zone (Beck and Nelson, 1996). For example, in MDCK cells, the basolateral membrane protein Na/K-ATPase accumulates within the contact zone, whereas the apical membrane protein gp135 is excluded (Wang *et al*., 1990). The accumulation of the Na/K-ATPase at the cell surface into the contact zone was shown to be a consequence of its attachment to the rearranging actin cytoskeleton, and thus resulted in its exclusion from internalization (Hammerton *et al*., 1991). Similarly, we show that expression of EFA6A promotes the selective cell surface retention of TJ proteins and their exclusion from endocytosis. We also show that EFA6A expression stabilizes the TJ proteins, but not E-cadherin, at the cell surface associated to the actin cytoskeleton as judged by Triton X-100 insolubility. We conclude that the stabilizing effect of EFA6A on the apical actin cytoskeleton accounts for the faster formation of the TJ that we observed during calcium switch experiments.

Although, the expression of EFA6A in fully polarized cells does not affect the morphology nor the barrier function of the TJ, it increases TJ stability as indicated by the latrunculin and calcium removal experiments. A variety of physiological agonists and pathological conditions that influence junctional permeation through effects on the cytoskeleton have been reported (Mitic and Anderson, 1998; Nusrat *et al*., 2000; Turner, 2000). In this context, EFA6, besides its implication in TJ biogenesis, could play a major role at steady state to regulate the interactions between the TJ and its associated acto-myosin cytoskeleton. It is also becoming increasingly clear that TJs are highly dynamic structures whose barrier function can be affected independently of E-cadherin by a large variety of physiological and pathological regulation (Balda and Matter, 1998; Mitic and Anderson, 1998; Cereijido *et al*., 2000). Therefore, it is possible that EFA6 could be activated and/or recruited by other signaling pathways to regulate TJ.

Recent studies using MDCK cells characterized a few other regulatory molecules that impact the assembly without seemingly affecting the overall steady-state morphology and/or function of the TJs in a polarized monolayer. These include the small G protein cdc42 (Rojas *et al*., 2001), the aPKC (Suzuki *et al*., 2001), and Par3 (Hirose *et al*., 2002) molecules that are part of the evolutionarily conserved Par3–aPKC–Par6 complex (Ohno, 2001). The effects on TJs of EFA6 seem similar to the one reported for each member of the Par3–aPKC–Par6–cdc42(GTP) complex; therefore, it is tempting to speculate that EFA6 would participate in TJ biogenesis at the same stage as the Par complex, as well as cdc42 and could act along or would be part of, the same pathway.

ACKNOWLEDGMENTS

We thank Drs. S. Tsukita, W. Gallin, G. Ojakian, and K. Matlin for the kind gifts of antibodies. We are grateful to Dr. P. Chavrier and T. Dubois for sharing reagents and expertise for the Arf6 pull-down assay before publication. We are indebted to Dr. K.L. Singer for stimulating discussions and critical review of the manuscript. We also thank Mariagrazia Partisani for technical skills. This work was supported by a grant from the Ligue Nationale Française Contre le Cancer.

REFERENCES

Altschuler, Y., Liu, S.-H., Katz, L., Tang, K., Hardy, S., Brodsky, F., Apodaca, G., and Mostov, K. (1999). ADP-ribosylation factor 6 and endocytosis at the apical surface of Madin-Darby canine kidney cells. J. Cell Biol. *147*, 7–12.

Balda, M.S., and Matter, K. (1998). Tight junctions. J. Cell Sci. *111*, 541–547.

Beck, K.A., and Nelson, W.J. (1996). The spectrin-based membrane skeleton as a membrane protein-sorting machinery. Am. J. Physiol. *270*, C1263–C1270.

Cereijido, M., Shoshani, L., and Contreras, R.G. (2000). Biogenesis of tight junctions and epithelial polarity. Am. J. Physiol. *279*, G477–G482.

Cereijido, M., Valdés, J., Shoshani, L., and Contreras, R.G. (1998). Role of tight junctions in establishing and maintaining cell polarity. Annu. Rev. Physiol. *60*, 161–177.

Chavrier, P., and Goud, B. (1999). The role of ARF and Rab GTPases in membrane transport. Curr. Opin. Cell Biol. *11*, 466–475.

Denker, B.M., and Nigam, S.K. (1998). Molecular structure and assembly of the tight junction. Am. J. Physiol. *274*, F1–F9.

Derrien, V., Couillault, C., Franco, M., Martineau, S., Montcourrier, P., Houlgatte, R., and Chavrier, P. (2002). A conserved C-terminal domain of EFA6-family ARF6-guanine nucleotide exchange factors induces lengthening of microvilli-like membrane protrusions. J. Cell Sci. *115*, 2867–2879.

Drubin, D.G., and Nelson, W.J. (1996). Origins of cell polarity. Cell *84*, 335–344.

Franco, M., Peters, P.J., Boretto, J., van Donselaar, E., Neri, A., D'Souza-Schorey, C., and Chavrier, P. (1999). EFA6, a sec7 domain-containing exchange factor for ARF6, coordinates membrane recycling and actin cytoskeleton organization. EMBO J. *18*, 1480–1491.

Frank, S., Upender, S., Hansen, S.H., and Casanova, J.E. (1998). ARNO is a guanine nucleotide exchange factor for ADP-ribosylation factor 6. J. Biol. Chem. *273*, 23–27.

Furuse, M., Fujita, K., Hiiragi, T., Fujimoto, K., and Tsukita, S. (1998). Claudin-1 and -2, novel integral membrane proteins localizing at tight junctions with no sequence similarity to occludin. J. Cell Biol. *141*, 1539–1550.

Furuse, M., Hirase, T., Itoh, M., Nagafuchi, A., Yonemura, S., Tsukita, S., and Tsukita, S. (1993). Occludin: a novel integral membrane protein localizing at tight junctions. J. Cell Biol. *123*, 1777–1788.

Gronewold, T.M., Sasse, F., Lunsdorf, H., and Reichenbach, H. (1999). Effects of rhizopodin and latrunculin B on the morphology and on the actin cytoskeleton of mammalian cells. Cell Tissue Res. *295*, 121–129.

Gumbiner, B.M. (1996). Cell adhesion: the molecular basis of tissue architecture and morphogenesis. Cell *84*, 354–357.

Hall, A. (1998). Rho GTPases and the actin cytoskeleton. Science *279*, 509–514.

Hammerton, R.W., Krzeminski, K.A., Mays, R.W., Ryan, T.A., Wollner, D.A., and Nelson, W.J. (1991). Mechanisms for regulating cells surface distribution of Na^+, K^+-ATPase in polarized epithelial cells. Science *254*, 847–850.

Hirose, T., *et al*. (2002). Involvement of ASIP/PAR-3 in the promotion of epithelial tight junction formation. J. Cell Sci. *115*, 2485–2495.

Izumi, Y., Hirose, T., Tamai, Y., Hirai, S., Nagashima, Y., Fujimoto, T., Tabuse, Y., Kemphues, K.J., and Ohno, S. (1998). An atypical PKC directly associates and colocalizes at the epithelial tight junction with ASIP, a mammalian homologue of *Caenorhabditis elegans* polarity protein PAR-3. J. Cell Biol. *143*, 95–106.

Jackson, C.L., and Casanova, J.E. (2000). Turning on ARF: the Sec7 family of guanine-nucleotide-exchange factors. Trends Cell Biol. *10*, 60–67.

Joberty, G., Petersen, C., Gao, L., and Macara, I.G. (2000). The cell-polarity protein Par6 links Par3 and atypical protein kinase C to Cdc42. Nat. Cell Biol. *2*, 531–539.

Jou, T.-S., and Nelson, W.J. (1998). Effects of regulated expression of mutant RhoA and Rac1 small GTPases on the development of epithelial (MDCK) cell polarity. J. Cell Biol. *142*, 85–100.

Jou, T.-S., Schneeberger, E.E., and Nelson, W.J. (1998). Structural and functional regulation of tight junctions by RhoA and Rac1 small GTPases. J. Cell Biol. *142*, 101–115.

Knust, E., and Bossinger, O. (2002). Composition and formation of intercellular junctions in epithelial cells. Science *298*, 1955–1959.

Londono, I., Marshansky, V., Bourgoin, S., Vinay, P., and Bendayan, M. (1999). Expression and distribution of adenosine diphosphate-ribosylation factors in the rat kidney. Kidney Int. *55*, 1407–1416.

Macia, E., Chabre, M., and Franco, M. (2001). Specificities for the small G proteins ARF1 and ARF6 of the guanine nucleotide exchange factors ARNO and EFA6. J. Biol. Chem. *276*, 24925–24930.

Marshansky, V., Bourgoin, S., Londoño, I., Bendayan, M., and Vinay, P. (1997). Identification of ADP-ribosylation factor-6 in brush-border membrane and early endosomes of human kidney proximal tubules. Electrophoresis *18*, 538–547.

Mitic, L.L., and Anderson, J.M. (1998). Molecular architecture of tight junctions. Annu. Rev. Physiol. *60*, 121–142.

Mooseker, M.S. (1985). Organization, chemistry, and assembly of the cytoskeletal apparatus of the intestinal brush border. Annu. Rev. Cell Biol. *1*, 209–241.

Niedergang, F., Colucci-Guyon, E., Dubois, T., Raposo, G., and Chavrier, P. (2003). ADP ribosylation factor 6 is activated and controls membrane delivery during phagocytosis in macrophages. J. Cell Biol. *161*, 1143–1150.

Nusrat, A., Turner, J.R., and Madara, J.L. (2000). Molecular physiology and pathophysiology of tight junctions. IV. Regulation of tight junctions by extracellular stimuli: nutrients, cytokines, and immune cells. Am. J. Physiol. *279*, G851–G857.

Ohno, S. (2001). Intercellular junctions and cellular polarity: the PAR-aPKC complex, a conserved core cassette playing fundamental roles in cell polarity. Curr. Opin. Cell Biol. *13*, 641–648.

Palacios, F., Price, L., Schweitzer, J., Collard, J.G., and D'Souza-Schorey, C. (2001). An essential role for ARF6-regulated membrane traffic in adherens junction turnover and epithelial cell migration. EMBO J. *20*, 4973–4986.

Palacios, F., Schweitzer, J.K., Boshans, R.L., and D'Souza-Schorey, C. (2002). ARF6-GTP recruits Nm23–H1 to facilitate dynamin-mediated endocytosis during adherens junctions disassembly. Nat. Cell Biol. *11*, 11.

Radhakrishna, H., Klausner, R.D., and Donaldson, J.G. (1996). Aluminum fluoride stimulates surface protrusions in cells overexpressing the ARF6 GTPase. J. Cell Biol. *134*, 935–947.

Roh, M. H., Fan, S., Liu, C.-J., and B., M. (2003). The Crumbs3-Pals1 complex participates in the establishment of polarity in mammalian epithelial cells. J. Cell Sci. *116*, 2895–2906.

Rojas, R., Ruiz, W.G., Leung, S.-M., Jou, T.-S., and Apodaca, G. (2001). Cdc42-dependent modulation of tight junctions and membrane protein traffic in polarized Madin-Darby canine kidney Cells. Mol. Biol. Cell *12*, 2257–2274.

Saitou, M., Fujimoto, K., Doi, Y., Itoh, M., Fujimoto, T., Furuse, M., Takano, H., Noda, T., and Tsukita, S. (1998). Occludin-deficient embryonic stem cells can differentiate into polarized epithelial cells bearing tight junctions. J. Cell Biol. *1998*, 397–408.

Sakakibara, A., Furuse, M., Saitou, M., Ando-Akatsuka, Y., and Tsukita, S. (1997). Possible involvement of phosphorylation of occludin in tight junction formation. J. Cell Biol. *137*, 1393–1401.

Santy, L.C. (2002). Characterization of a fast cycling ADP-ribosylation factor 6 mutant. J. Biol. Chem. *277*, 40185–40188.

Santy, L.C., and Casanova, J.E. (2001). Activation of ARF6 by ARNO stimulates epithelial cell migration through downstream activation of both Rac1 and phospholipase D. J. Cell Biol. *154*, 599–610.

Schmidt, A., and Hall, A. (2002). Guanine nucleotide exchange factors for Rho GTPases: turning on the switch. Genes Dev. *16*, 1587–1609.

Schneeberger, E.E., and Lynch, R.D. (1992). Structure, function, and regulation of cellular tight junctions. Am. J. Physiol. *262*, L6647–L6661.

Spector, I., Shochet, N.R., Kashman, Y., and Groweiss, A. (1983). Latrunculins: novel marine toxins that disrupt microfilament organization in cultured cells. Science *219*, 493–495.

Stevenson, B.R., Anderson, J.M., and Bullivant, S. (1988). The epithelial tight junction: structure, function and preliminary biochemical characterization. Mol. Cell. Biochem. *83*, 129–145.

Stevenson, B.R., Siliciano, J.D., Mooseker, M.S., and Goodenough, D.A. (1986). Identification of ZO-1, a high molecular weight polypeptide associated with the tight junction (zonula occludens) in a variety of epithelia. J. Cell Biol. *103*, 755–766.

Suzuki, A., Yamanaka, T., Hirose, T., Manabe, N., Mizuno, K., Shimizu, M., Akimoto, K., Izumi, Y., Ohnishi, T., and Ohno, S. (2001). Atypical protein kinase C is involved in the evolutionarily conserved par protein complex and plays a critical role in establishing epithelia-specific junctional structures. J. Cell Biol. *152*, 1183–1196.

Tsukita, S., Furuse, M., and Itoh, M. (2001). Multifunctional strands in tight junctions. Nat. Mol. Cell. Biol. *2*, 285–293.

Turner, J.R. (2000). 'Putting the squeeze' on the tight junction: understanding cytoskeletal regulation. Semin. Cell Dev. Biol. *11*, 301–308.

Vetter, I.R., and Wittinghofer, A. (2001). The guanine nucleotide-binding switch in three dimensions. Science *294*, 1299–1304.

Wang, A.Z., Ojakian, G.K., and Nelson, W.J. (1990). Steps in the morphogenesis of a polarized epithelium. I. Uncoupling the roles of cell-cell and cell-substratum contact in establishing plasma membrane polarity in multicellular epithelial (MDCK) cysts. J. Cell Sci. *95*, 137–151.

Wong, V. (1997). Phosphorylation of occludin correlates with occludin localization and function at the tight junction. Am. J. Physiol. *273*, C1859–C1867.

Zahraoui, A., Louvard, D., and Galli, T. (2000). Tight junction, a platform for trafficking and signaling protein complexes. J. Cell Biol. *151*, 31–36.